

Narrow spectral band monolithic lead-chalcogenide-on-Si mid-IR photodetectors

H. ZOGG* and M. ARNOLD

Thin Film Physics Group, Laboratory for Solid State Physics, Swiss Federal Institute of Technology (ETH),
1 Technopark Str., CH-8005 Zurich, Switzerland

Narrow spectral band infrared detectors are required for multispectral infrared imaging. Wavelength selectivity can be obtained by placing passive line filters in front of the detectors, or, the preferred choice, by making the detectors themselves wavelength selective. We review the first photovoltaic resonant cavity enhanced detectors (RCED) for the mid-IR range. The lead-chalcogenide (PbEuSe) photodetector is placed as a very thin layer inside an optical cavity. At least one side is terminated with an epitaxial Bragg mirror (consisting of quarter wavelength PbEuSe/BaF₂ pairs), while the second mirror may be a metal. Linewidths are as narrow as 37 nm at a peak wavelength of 4400 nm, and peak quantum efficiencies up to above 50% are obtained.

Keywords: infrared sensors, resonant cavity, lead-chalcogenides, molecular beam epitaxy, silicon substrates.

1. Introduction

The most sensitive detectors for the mid-infrared range (3–20 μm) are obtained with narrow gap semiconductors (NGS) [1,2]. These detectors have a broad spectral sensitivity up to the cut-off wavelength which is determined by the (narrow) band gap. The quantum efficiency is high due to the direct band gap. Large focal plane arrays (FPAs) in one or two dimensions are fabricated for various applications. Preferred materials are HgCdTe and InSb. The IR-FPAs are typically fabricated in a hybrid structure: A NGS-chip containing the IR-sensors is mated to the Si-read-out chip with In-bumps. Narrow gap lead-chalcogenides (PbSnX, PbEuX, X = Se,Te) may be applied, too, for this purpose, but not many groups are presently working on this topic. Here, Si-substrates are used onto which the lead-chalcogenide is grown by molecular beam epitaxy (MBE). This is possible despite the huge lattice- and thermal expansion mismatch, photovoltaic lead-chalcogenide sensors are rather tolerant to structural defects (in contrast to the HgCdTe or InSb material families). Lead-chalcogenide IR-arrays have been fabricated with cut-off wavelengths ranging from 3 to 12 μm [2]. The Si-substrate may even contain the read-out electronics: A two dimensional monolithic array with 96×128 pixels for the 3–5 μm range has been realized [3].

In addition to single colour IR-FPAs, multispectral or even hyperspectral sensor arrays for enhanced object discrimination operating in different bands and/or narrow lines are needed today [4]. Preferably, the detector array it-

self is able to discriminate the spectral ranges rather than to employ passive filters in front of the array. The spectral bands or narrow lines should preferentially be tunable depending on the application.

Here, we describe narrow spectral band infrared detectors based on monolithic resonant cavities which exhibit sensitivity in a very narrow spectral band only. For the first time, high quantum efficiencies and single narrow line widths have been obtained in the mid-IR range.

They are realised with epitaxial narrow gap lead-chalcogenide layers which are especially suited for this purpose:

- cut-off wavelengths between 3 and > 15 μm are obtained by chemical tuning [2,3]. The cut-off wavelength of PbSe at 100 K is 6.9 μm . In ternary Pb_{1-x}Eu_xSe alloys, the cut-off wavelength decreases with increasing Eu content, while with Pb_{1-x}Sn_xSe compositions higher cut-off wavelengths result with increasing Sn content. Note that in addition the bandgap of IV–VI materials and therefore the cut-off wavelengths significantly change with temperatures (for PbSe, 8 μm at 40 K and 4.4 μm at 300 K).
- distributed Bragg reflectors (DBR) with high reflectivities are easily obtained with only a few $\lambda/4$ quarter wavelengths layer pairs with alternating high H and low L refractive indices. Typical combinations are PbEuSe/EuSe [5] or PbEuSe/BaF₂ [6]. This is because the refractive index of the H layer (PbEuSe) is as high as $n_H \cong 5$, while that of the L layers are low ($n_L = 2.4$ for EuSe, $n_L = 1.43$ for BaF₂). With such large H/L contrasts, one to three H/L pairs already give high reflectivities. Note that with III–V or II–VI materials, a much larger number of H/L pairs is needed for high reflectivity due to the much lower n_H/n_L ratio.

* e-mail: zogg@phys.ethz.ch

The paper presented there appears in *Infrared Photoelectronics*, edited by Antoni Rogalski, Eustace L. Dereniak, Fiodor F. Sizov, Proc. SPIE Vol. 5957, 59570B (2005).

- lead-chalcogenide materials are “forgiving”, IR-devices with sufficient quality result even in materials containing a considerable number of dislocations. This allows lattice-mismatched growth by molecular beam epitaxy even on Si-substrates.
- Pb/PbXSe (X = Eu,Sn) metal/semiconductor contacts yield high quality photovoltaic IV–VI detectors. Whole large focal plane arrays even on active Si-chips containing read-out electronics have been fabricated with this technology [3].

We already published the first results on these sensors demonstrating a single narrow line with high peak quantum efficiency [7]. With HgCdTe and GaSb RCEDs, simulations have been published [8,9], and preliminary structures have been realized with InAs [10]. With lead-chalcogenides, first results of photoconductive sensors are available, too [11].

2. RCED principle

As shown in Fig. 1, resonant cavity enhanced detectors (RCEDs) consist of a Fabry-Perot cavity with front and back end terminated by high reflectivity mirrors [12]. At

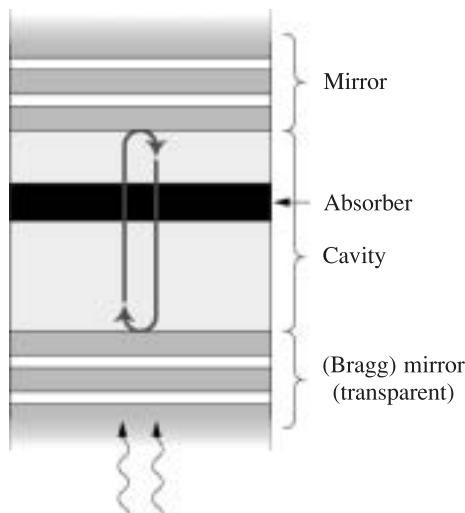


Fig. 1. Principle of a RCED.

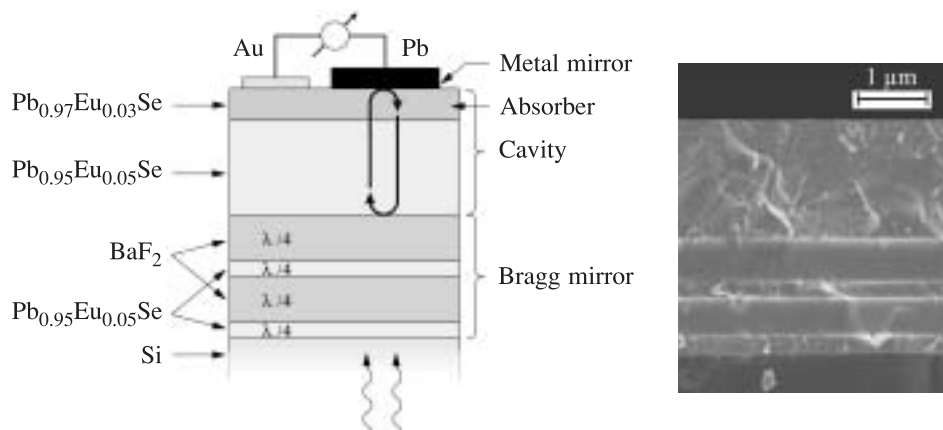


Fig. 2. Schematic cross section of a lead-chalcogenide RCED and corresponding scanning electron microscopic image.

the cavity resonance wavelengths, photons enter the cavity and may cycle back and forth many time before they are absorbed in the detector (absorber) layer. The optical length of the cavity determines the resonance wavelengths, and the finesse the widths of the resonances. If the front and back mirrors have high reflectivities and the absorption inside the cavity is low, the finesse is high and therefore a very narrow line width is obtained. High quantum efficiencies result even for very thin absorber layers in this case because of the photon recycling effect. In addition, the thin detector layer may result in a much lower noise than in non-cavity broad band detectors since the absorption thickness and therefore the detector volume is small, leading to lower generation-recombination noise.

3. Design and fabrication

As shown in Fig. 2, the light enters through the bottom DBR which consists just of two pairs of $\text{Pb}_{1-x}\text{Eu}_x\text{Se}/\text{BaF}_2$ layers. This mirror is nonabsorbing at the design wavelength ($4.4 \mu\text{m}$). It is followed by a nonabsorbing $\text{Pb}_{1-x}\text{Eu}_x\text{Se}$ spacer layer and the thin absorbing $\text{Pb}_{1-y}\text{Eu}_y\text{Se}$ ($y < x$) detector layer. The 5th order resonance was chosen for the present design. The top mirror consists of Pb which in addition forms the photovoltaic detector with the absorber layer. The thickness of this $\text{Pb}_{1-y}\text{Eu}_y\text{Se}$ absorber/detector layer is chosen in a way that it extends to near an antinode of the standing wave inside the cavity, therefore leading to high quantum efficiency.

The calculated reflectivities are 95% for the DBR and 98% for the Pb mirror. The latter was obtained by fitting reflection spectra, since tabulated reflectivities of Pb are not reliable and depend on the layer preparation and history.

The layers are grown on a Si(111) substrate in a 2-chamber MBE system as described elsewhere [13]. A thin (2 nm) CaF_2 buffer is grown first on the Si-substrate for compatibility. The right part of Fig. 2 shows a cleaved cross section of the structure.

3. Example of a device with 4.4- μm peak wavelength

The measured spectral response of the device described above is shown in Fig. 3. The linewidth is as narrow 0.8%, while the peak quantum efficiency exceeds 30%. No antireflection coating was applied, with an ideal AR coating around 40% would result. The peak visible corresponds to 5th order. Resonance peaks of other orders are not visible, lower order (longer wavelengths) resonance peaks are above the cut-off wavelength of the absorber and are therefore not detected. For higher order peaks (6th and higher), the DBR mirror and/or spacer layer already absorbs this radiation resulting in a very low response for these peaks.

Sensitivities (in term of inverse noise currents or resistance-area RoA products) are around 300 Ωcm^2 at 100 K, and 60 Ωcm^2 at 180 K. These values are above the background noise limit for a broad band detector and room temperature background radiation, but of course still far below the theoretical diffusion limit of lead-chalcogenide detectors.

The peak wavelength λ_p is given by the optical thickness of the cavity. Care has to be taken to chose suitable compositions of the spacer and absorber layers. The cut-off wavelength λ_c of the absorber has to be slightly longer than λ_p in order that no lower resonance orders give rise to a photocurrent and to obtain highest sensitivity at the design temperature. This is easily achieved by choosing $\text{Pb}_{1-x}\text{Y}_x\text{Se}$ ($\text{Y} = \text{Eu}, \text{Sn}$) with the right composition x , however.

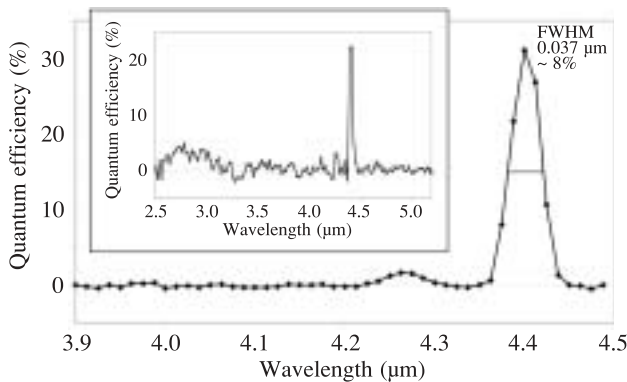


Fig. 3. Spectral response of a $\text{Pb}_{0.965}\text{Eu}_{0.035}\text{Se}$ RCED. The resonance peak at 4.4 μm has a width as low as 0.8% while the quantum efficiency is > 30% (without AR coating).

4. Voltage tunability

If a reverse voltage is applied, sensitivity at lower wavelengths develops in addition to the narrow peak (at 3.9 μm for the device in Fig. 4). This results in a voltage tunable two-colour sensor. The broad low wavelength peak is due to absorption in the PbEuSe spacer layer. At a large enough reverse voltage, the depletion zone is extended into the PbEuSe spacer layer. Carriers generated in this layer may reach the junction and give rise to the broad plateau ranging from 3–3.7 μm wavelength. In Fig. 5, the spectral absorption is simulated.

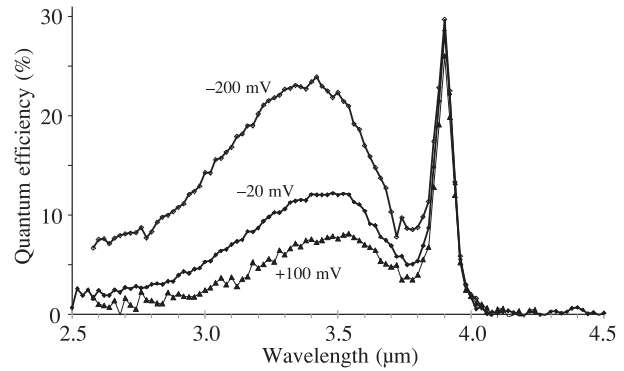


Fig. 4. Voltage tunability of a RCED. By applying a reverse voltage to the absorber, the depletion width may be extended until it reaches the spacer layer. This results in an additional response below the peak wavelength $T = 100\text{ K}$.

The field strength and the absorption as a function of the incoming wavelength and the position in the device are calculated. From the integration of the absorption over the spatial range, from which the photogenerated electrons reach the junction, the response is calculated.

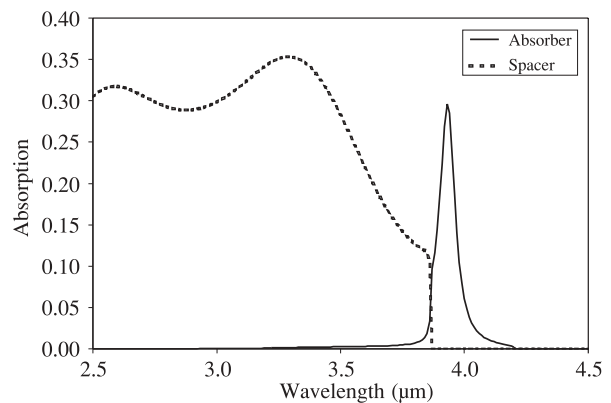


Fig. 5. Simulated absorption in the absorber and spacer layer of a RCED with a design wavelength of 3.9 μm .

5. Device with 7.3- and/or 8.4- μm wavelengths

This RCED is designed for 7.3 μm peak wavelength. $\text{Pb}_{0.965}\text{Sn}_{0.035}\text{Se}$ forms the absorber and PbSe is used as spacer layer as well as for the high index part of the bottom Bragg mirror. Only one pair of quarter wavelength layers was used in the front mirror. Again, the cutoff wavelength of the PbSe in the front mirror and in the spacer is chosen in order to absorb the unwanted higher mode resonances, while lower mode resonances should not be detected because their wavelength is longer than the cut-off wavelength of the absorber.

According to Fig. 6, two dominant response peaks are observed at 7.3 μm and at 8.4 μm , however. The linewidths are 0.22 μm and 0.24 μm ($\Delta\lambda/\lambda \cong 2.9\%$). The quantum efficiency is above 50%. No antireflection coating was applied.

If only one spectral peak is desired, this can be achieved as follows. The peak at 8.4 μm might be suppressed by lower-

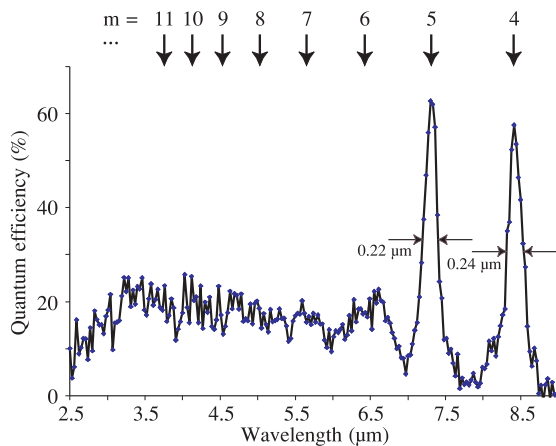


Fig. 6. Measured spectral response of a $\text{Pb}_{0.965}\text{Sn}_{0.035}\text{Se}$ -RCED designed for $7.3 \mu\text{m}$. The arrows indicate the resonant wavelengths of the different orders m . $T = 100 \text{ K}$.

ing the cut-off wavelength by using less Sn in the absorber layer, or by running the detector at higher temperatures where the cut-off wavelength decreases to below $8.2 \mu\text{m}$. Alternatively, the peak at $7.3 \mu\text{m}$ might be suppressed by the addition of about 2.5% Sn into the mirror and the spacer layer of the cavity in order to absorb this shorter wavelength radiation.

6. Mechanical tunability

The peak wavelength is determined by the optical thickness of the cavity. If this thickness can be varied, a large spectral tunability results. In Fig. 7, a possible solution is shown: The bottom Bragg mirror, spacer and detector layer are designed as before. The top mirror, however, is separated from the bottom part and can be mechanically displaced with the aid of a Si-micromechanics structure. This changes the optical cavity length. In order that the structure remains transparent, a p-n rather than a metal/semiconductor junction has now to be employed as photovoltaic detector. This results in a slightly more complicated design, but lead-chalcogenide p-n junctions may be fabricated, too [3]. In addition, an antireflection coating has to be applied. Work is ongoing to realize such a structure.

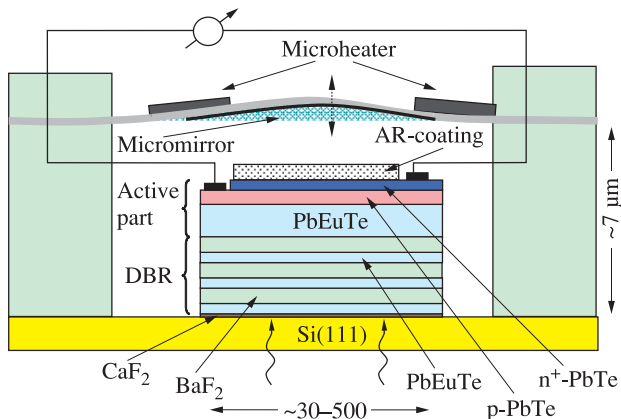


Fig. 7. A possible mechanically tunable RCED with a movable top mirror realised with Si-micromechanics.

7. Conclusions

Resonant cavity enhanced detectors (RCED) with high quantum efficiencies and one single narrow spectral line have been realised for the first time in the mid-IR range. The detectors consist of narrow gap lead-chalcogenides grown on Si-substrates. The high ratios of the refractive indices of the materials employed ($n_H \cong 5$ for $\text{Pb}_{1-x}\text{Eu}_x\text{Se}$, $n_L \cong 1.4$ for BaF_2) facilitate obtaining distributed Bragg mirrors which yield high reflectivities with only a few quarter wavelength H/L pairs for this case.

The peak wavelength is determined by the design of the cavity and may be chosen anywhere between $3 \mu\text{m}$ and $> 15 \mu\text{m}$ by using appropriate compositions $\text{Pb}_{1-x}\text{Y}_x\text{Se}$ ($Y = \text{Eu, Sn}$) of the absorber layer. Applications are for IR-hyperspectral imaging as well as for spectroscopy.

References

1. A. Rogalski, K. Adamiec, and J. Rutkowski, *Narrow-Gap Semiconductor Photodiodes*, SPIE Press, Bellingham, 2000.
2. *Infrared Detectors and Emitters: Material and Devices*, edited by P. Capper, C.T. Elliott, Kluwer Academic Publ., Boston/Dordrecht/London, 2000.
3. H. Zogg, K. Alchalabi, D. Zimin, and K. Kellermann, "Two-dimensional monolithic lead chalcogenide infrared sensor arrays on silicon read-out chips and noise mechanisms", *IEEE Trans. Electron Devices* **50**, 209-214 (2003).
4. J. Carrano, J. Brown, P. Percont, and K. Barnard, "Tuning in to detection", *SPIE OE magazine*, 20-22 (2004).
5. W. Heiss, M. Böberl, T. Schwarzl, G. Springholz, J. Fürst and H. Pascher, "Applications of lead-salt microcavities for mid-infrared devices," *IEE Proc. Optoelectron.* **150**, 332-336 (2003).
6. F. Zhao, H. Wu, A. Majumdar, and Z. Shi, "Continuous wave optically pumped lead-salt mid-infrared quantum-well vertical-cavity surface-emitting lasers", *Appl. Phys. Lett.* **83**, 5133 (2003).
7. M. Arnold, D. Zimin, K. Alchalabi and H. Zogg, "Lead salt mid-IR photodetectors with narrow linewidth," *J. Cryst. Growth* **278**, 739-742 (2005).
8. J.G.A. Wehner, T.N. Nguyen, J. Antoszewski, C.A. Musca, J.M. Dell, and L. Faraone, "Resonant cavity-enhanced mercury cadmium telluride detectors", *J. Electronic Materials* **33**, 604-608 (2004).
9. L. Jun, S. Hang, Y. Jin, J. Hong, G. Miao, and H. Zhao, "Design of a resonant-cavity-enhanced GaInAsSb/GaSb photodetector", *Semicond. Sci. Technol.* **19**, 690-694 (2004).
10. A.M. Green, D.G. Gevaux, C. Roberts, P.N. Stavrinou, and C.C. Phillips, " $\lambda \approx 3 \mu\text{m}$ InAs resonant-cavity-enhanced photodetector", *Semicond. Sci. Technol.* **18**, 964-967 (2003).
11. M. Böberl, T. Fromherz, T. Schwarzl, G. Springholz, and W. Heiss, "IV-VI resonant-cavity enhanced photodetectors for the mid-infrared", *Semicond. Sci. Technol.* **19**, L115-L117 (2004).
12. M.S. Ünlü and S. Strite, "Resonant cavity enhanced photonic devices", *J. Appl. Phys.* **78**, 607-639 (1995).
13. D. Zimin, "Growth and properties of optoelectronic structures based on IV-VI materials," *Diss. ETH Nr. 15733*, Zurich, 2004.